



Contents lists available at SciVerse ScienceDirect

## Spectrochimica Acta Part A: Molecular and Biomolecular Spectroscopy

journal homepage: [www.elsevier.com/locate/saa](http://www.elsevier.com/locate/saa)

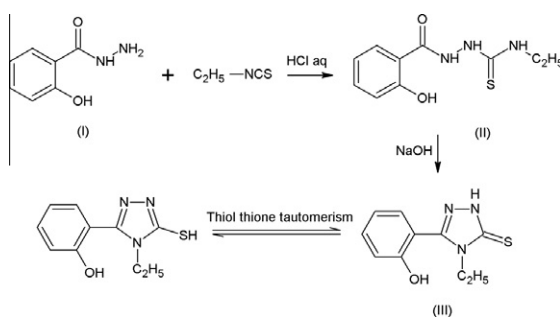
## Synthesis, experimental, theoretical characterization and biological activities of 4-ethyl-5-(2-hydroxyphenyl)-2H-1,2,4-triazole-3(4H)-thione

Metin Koparir<sup>a,\*</sup>, Cahit Orek<sup>a</sup>, Pelin Koparir<sup>b</sup>, Kamiran Sarac<sup>c</sup><sup>a</sup> Firat University, Faculty of Science, Department of Chemistry, 23119 Elazig, Turkey<sup>b</sup> Department of Chemistry, Forensic Medicine Institute, TR-44000 Malatya, Turkey<sup>c</sup> İnönü University, Faculty of Science, Department of Chemistry, 44100 Malatya, Turkey

## HIGHLIGHTS

- ▶ 4-Ethyl-5-(2-hydroxyphenyl)-2H-1,2,4-triazole-3(4H)-thione was prepared.
- ▶ Synthesis compound was confirmed by IR, NMR and X-ray single-crystal diffraction.
- ▶ Experimental parameters of title compound were compared with calculated parameters.
- ▶ The title compound has been tested in vitro for biological effects.

## GRAPHICAL ABSTRACT



## ARTICLE INFO

## Article history:

Received 30 October 2012

Received in revised form 10 December 2012

Accepted 14 December 2012

Available online 2 January 2013

## Keywords:

4-Ethyl-5-(2-hydroxyphenyl)-2H-1,2,4-triazole-3(4H)-thione

DFT

NMR

IR spectra

Biological effects

## ABSTRACT

This work presents the characterization of 4-ethyl-5-(2-hydroxyphenyl)-2H-1,2,4-triazole-3(4H)-thione (**III**) by quantum chemical calculations and spectral techniques. The molecular geometry, vibrational frequencies and gauge including atomic orbital (GIAO) <sup>1</sup>H and <sup>13</sup>C NMR chemical shift values of **III** in the ground state have been calculated using the density functional method (B3LYP) with the 6-31G(d) basis set. The calculated results show that the optimized geometry can well reproduce the crystal structure, and the theoretical vibrational frequencies and chemical shift values show good agreement with experimental values. To determine conformational flexibility, the molecular energy profile of the title compound was obtained by DFT calculations with respect to the selected torsion angle, which was varied from  $-180^\circ$  to  $+180^\circ$  in steps of  $10^\circ$ . The energetic behavior of **III** in solvent media was examined using the B3LYP method with the 6-31G(d) basis set by applying the Onsager and the polarizable continuum model (PCM). The predicted nonlinear optical properties of **III** are greater than ones of urea. In addition, DFT calculations of molecular electrostatic potentials and frontier molecular orbitals of **III** were carried out at the B3LYP/6-31G(d) level of theory. The title compound was screened for antibacterial, antifungal and antioxidant activities.

© 2012 Elsevier B.V. All rights reserved.

## Introduction

1,2,4-triazole rings are typically planar  $6\pi$ -electron aromatic systems, featuring an extensive chemistry [1,2]. 1,2,4-triazole and its derivatives represent one of the most biologically active classes of compounds, possessing a wide spectrum of activities,

including anti-inflammatory [3,4], antiviral [5], analgesic [6], antimicrobial [7], anticonvulsant [8], anticancer [9], antioxidant [10], antitumoral [11] and antidepressant activity [12], the last usually being explored by the forced-swim test [13,14]. Furthermore, some of the complexes containing 1,2,4-triazole ligands have rather peculiar structures and specific magnetic properties [15–18].

4,5-Substituted products containing 1,2,4-triazole ring in their structure seem to be suitable candidates for further chemical modifications and might be of interest as pharmacologically active

\* Corresponding author. Tel.: +90 424 237 00 00; fax: +90 424 237 00 10.

E-mail address: [mkoparir@hotmail.com](mailto:mkoparir@hotmail.com) (M. Koparir).

compounds and useful ligands in coordination chemistry [19]. Derivatives of 4-amino-5-substituted 1,2,4-triazole were synthesized by intramolecular cyclization of 1,4-disubstituted thiosemicarbazides [20]. In addition there are some studies on electronic structures and thiol–thione tautomeric equilibrium of heterocyclic thione derivatives [21–25]. Several heterocycles containing a thiazole or triazole moiety have been reported; [26–30] however, the synthesis of heterocyclic systems containing a phenol-substituted triazole ring has rarely been reported [31–33].

Density functional theory (DFT) has been one of the widely used theories in theoretical modeling during recent years. By means of the development of better exchange–correlation functionals, it has become possible to calculate many molecular properties which have accuracies that can be comparable to traditionally correlated *ab initio* methods, all these could be done with more favorable computational costs [34]. It has been figured out during the literature survey that in reproducing the experimental values in geometry, dipole moment, vibrational frequency, etc. DFT has a precise accuracy [35–39].

The aim of this study is to investigate the energetic and structural properties of the 1,2,4-triazole compound, 4-ethyl-5-(2-hydroxyphenyl)-2H-1,2,4-triazole-3(4H)-thione (Fig. 1), using density functional theory calculations. In this study, the optimized geometry, vibrational spectra and assignments, statistical energetic parameters, conformational analysis and nonlinear optical properties of **III** have been studied. These calculations are valuable for providing insight into molecular properties of 1,2,4-triazole compounds. Besides the characterization of the title compound, the biological activities of the **III**, such as antibacterial, antifungal and antioxidant activities, were investigated.

## Experimental

### Synthesis

For the synthesis of 1(2-hydroxybenzoyl)-4-ethyl thiosemicarbazide (**II**), a mixture of **I** (0.01 mol) and ethyl isothiocyanate (0.01 mol) in absolute ethanol was refluxed for 8 h. The solid material obtained on cooling was filtered, washed with diethyl ether, dried and crystallized from ethanol–dioxane (yield 65%, m.p. 489–491 K). IR ( $\nu$ ,  $\text{cm}^{-1}$ ): 3495, 3317 (N–H, OH), 1668 (C=O), 1262 (C=S). For the synthesis of **III**, a stirred mixture of **II** (0.01 mol) and sodium hydroxide (40 mg, 0.01 mol, as a 2 N solution) was refluxed for 4 h. After cooling, the solution was acidified with HCl (37%) and the precipitate was filtered off. The precipitate was then crystallized from an ethanol–dioxane mixture (yield 85%, m.p. 527–531 K). IR ( $\nu$ ,  $\text{cm}^{-1}$ ): 3390, 3216 (N–H, O–H), 1622 (C=N), 1535, 1260, 1050, 950 (N–C=S, amide **I**, **II**, **III** and **IV** bands);  $^1\text{H}$  NMR (400 MHz, DMSO- $d_6$ , 24°C):  $\delta$  1.03 (t,  $J = 7.02$ , 3H,  $\text{CH}_3$ ), 3.47 (q,  $J = 7.32$ , 2H,  $\text{CH}_2$ ), 7.82–7.14 (m, 4H, Ar–H), 10.00 (s, 1H, OH), 13.80 (s, 1H, SH). Elemental analysis: C, 54.25; H, 5.05; N, 18.96.

### Physical measurements

Melting points were determined on a Thomas Hoover melting point apparatus and uncorrected, but checked by differential scanning calorimeter (DSC). KBr pellets on a Perkin–Elmer Spectrum

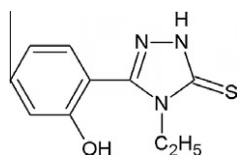


Fig. 1. Chemical diagram of 4-ethyl-5-(2-hydroxyphenyl)-2H-1,2,4-triazole-3(4H)-thione.

one FT-IR spectrophotometer was used in order to record FT-IR spectra of **III** in 4000–400  $\text{cm}^{-1}$  region. Electronic spectral studies were conducted on a Shimadzu model UV-1700 spectrophotometer in the wavelength 1100–200 nm. The  $^1\text{H}$  and  $^{13}\text{C}$  spectra were taken on Bruker AC-400 NMR spectrometer operating at 400 MHz for  $^1\text{H}$ –, 100 MHz for  $^{13}\text{C}$  NMR. Elemental analyses were done on a LECO-CHNS-938. Compound was dissolved in DMSO- $d_6$  and chemical shifts were referenced to TMS ( $^1\text{H}$  and  $^{13}\text{C}$  NMR). Starting chemicals were provided by Merck or Aldrich. The synthesis reaction of **III** is shown in Fig. 2.

### Antibacterial activity

The synthesized compound **III** was screened for their antibacterial activity against *Escherichia coli* (ATTC-25922), *Staphylococcus aureus* (ATTC-25923), *Pseudomonas aeruginosa* (ATCC-27853) and *Klebsiella pneumoniae* (recultured) bacterial strains by serial plate dilution method [40,41]. Serial dilutions of the drug in Muller–Hinton broth were taken in tubes and their pH was adjusted to 5.0 using phosphate buffer. Standardized suspension of the test bacterium was inoculated and incubated for 16–18 h at 37 °C. The minimum inhibitory concentration (MIC) was noted by observing the lowest concentration of the drug at which there was no visible growth. A number of antimicrobial disks are placed on the agar for the sole purpose of producing zones of inhibition in the bacterial lawn. Agar media were poured into each Petri dish. Excess of suspension was decanted and placing in incubator at 37 °C for 1 h dried the plates. Using an agar punch, wells were made on these seeded agar plates and minimum inhibitory concentrations of the test compounds in DMSO were added into each labeled well. A control was also prepared for the plates in the same way using DMSO as solvent. The Petri dishes were prepared in triplicate and maintained at 37 °C for 3–4 days. Antibacterial activity was determined by measuring the diameter of inhibition zone. Activity of each compound was compared with Ciprofloxacin as standard [42,43]. Zone of inhibition was determined for title compound the results are summarized in Table 1.

### Antifungal activity

Newly prepared compound was screened for their antifungal activity against *Aspergillus flavus* [NCIM No. 524], *Aspergillus fumigatus* [NCIM No. 902], *Penicillium marneffeii* [recultured] and *Trichophyton mentagrophytes* [recultured] in DMSO by serial plate dilution method [44,45]. Agar media were prepared by dissolving peptone (1 g), D-glucose (4 g) and agar (2 g) in distilled water (100 mL) and adjusting the pH to 5.7. Normal saline was used to make a suspension of spore of fungal strains for lawning. A loopful of particular fungal strain was transferred to 3 mL saline to get a suspension of corresponding species. Agar media of 20 mL were poured into each Petri dish. Excess of suspension was decanted and plates were dried by placing in an incubator at 37 °C for 1 h. Using an agar punch each labeled well were made on these seeded agar plates and MIC of the test compounds in DMSO were added into each labeled well. A control was also prepared for the plates in the same way using solvent DMSO. The Petri dish were prepared in triplicate and maintained at 37 °C for 3–4 days. Antifungal activity was determined by measuring the diameter of the inhibition zone. Activity of each compound was compared with Ciclopiroxolamine as standard. Zones of inhibition were determined for title compound the results are summarized in Table 2.

### DPPH free radical scavenging activity

Free radical scavenging activity of the title compound was determined by measuring the change in the absorbance of

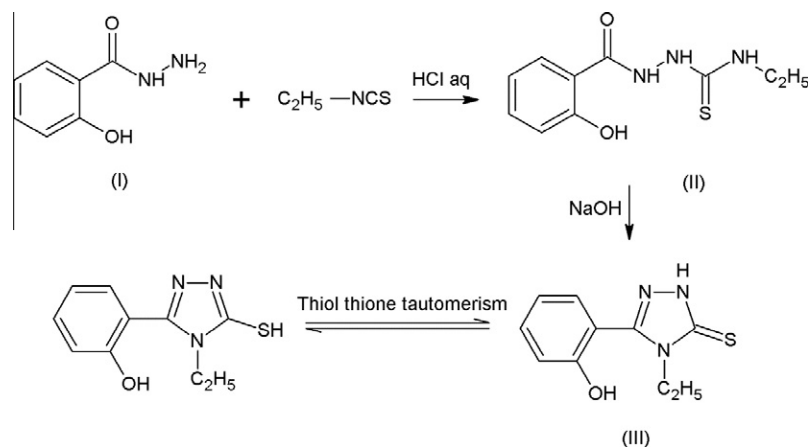


Fig. 2. The reaction for the synthesis of title compound.

Table 1

Minimum inhibitory concentration (MIC,  $\mu\text{g/mL}$ ) data of the title compound against a number of bacteria.

Compound	MIC in $\mu\text{g/mL}$ and zone of inhibition (mm)			
	<i>E. coli</i>	<i>K. pneumoniae</i>	<i>P. aeruginosa</i>	<i>S. aureus</i>
Title compound	6.25 (16–20)	12.50 (11–15)	12.50 (16–20)	6.25 (16–20)
Ciprofloxacin	6.25 (16–20)	6.25 (16–20)	6.25 (16–20)	1.56 (22–30)

Note: The MIC values were evaluated at concentration range, 1.56–25  $\mu\text{g/mL}$ .

Table 2

Antifungal activity of title compound.

Compound	MIC in $\mu\text{g/mL}$ and zone of inhibition (mm)			
	<i>P. marneffeii</i>	<i>T. mentagrophytes</i>	<i>A. flavus</i>	<i>A. fumigatus</i>
Title compound	12.50 (11–15)	6.25 (16–20)	6.25 (16–20)	12.50 (11–15)
Ciclopiroxolamine	6.25 (16–20)	3.125 (27–33)	3.125 (25–30)	6.25 (16–20)

Note: The MIC values were evaluated at concentration range, 1.56–25  $\mu\text{g/mL}$ .

DPPH $\cdot$  (1,1-diphenyl-2-picrylhydrazyl radical) at 517 nm spectrophotometrically. Stock solutions of 500  $\mu\text{M}$  of tested sample and DPPH $\cdot$  were prepared in DMSO. 400  $\mu\text{L}$  of DPPH $\cdot$  solution was added to sample solution at different concentrations (500, 1000, 1500, 2000 and 2500  $\mu\text{L}$ ) and appropriately diluted with DMSO to total volume of 4.0 mL. A 400  $\mu\text{L}$  from DPPH $\cdot$  stock solution was also diluted to 4.0 mL using DMSO as solvent to make the control. The reaction mixtures were thoroughly mixed by shaking the test tubes vigorously and incubated at 25  $^{\circ}\text{C}$  for 60 min in a water bath in the dark. Absorbance at 517 nm was measured and the solvent was corrected throughout. Ascorbic acid was used as a standard (using the reference antioxidant) for this test. The DPPH (1,1-diphenyl-2-picrylhydrazyl) radical scavenging method was chosen to determine the antioxidant potential of the target compounds in comparison with the commercially available antioxidant Ascorbic acid at the same concentrations. The scavenging effect was calculated using the following equation [46]:

$$\text{Scavenging activity (\%)} = \frac{A_0 - A_s}{A_0} \times 100$$

where  $A_s$  is the absorbance of the DPPH $\cdot$  in the presence of the tested compound and  $A_0$  is the absorbance of the DPPH $\cdot$  in the absence of the tested compound (control). The data for antioxidation presented as means  $\pm$  SD of three determinations.

### Computational methods

The molecular geometry was taken directly from the X-ray diffraction result unrestrainedly. In the following step, the Gaussian 09W software package [47] was used to make the DFT calculations with a hybrid functional B3LYP (Becke's Three parameter hybrid functional by means of the LYP correlation functional) with the 6-31G(d) basis set using the Berny method [48,49]. At the same level of the theory, the harmonic vibrational frequencies for the optimized structure were assessed and the frequencies obtained scaled by 0.9613 [50]. Gauss-View molecular visualization program was used to carry out vibrational band assignments [51]. Conformational energies were calculated as a one-dimensional scan by varying the  $\varphi_1(\text{N1}-\text{C1}-\text{C3}-\text{C4})$  and  $\varphi_2(\text{C1}-\text{N3}-\text{C9}-\text{C10})$  dihedral angles from  $-180^{\circ}$  to  $180^{\circ}$  in steps of  $10^{\circ}$ , and the molecular energy profile was obtained.

On order that we can evaluate the energetic and atomic charge behavior of **III** in solvent media, we performed optimization calculations in five solvent [ $\epsilon = 4.71$ , chloroform ( $\text{CHCl}_3$ );  $\epsilon = 10.13$ , dichloroethane ( $\text{CH}_2\text{ClCH}_2\text{Cl}$ );  $\epsilon = 24.85$ , ethanol ( $\text{C}_2\text{H}_5\text{OH}$ );  $\epsilon = 46.83$ , DMSO;  $\epsilon = 78.36$ , water ( $\text{H}_2\text{O}$ )]. These calculations were made at the B3LYP/6-31G(d) level and Onsager [52] and Polarizable Continuum Model (PCM) [53–56] methods were used. To investigate the reactive sites of **III** the molecular electrostatic potentials were evaluated using B3LYP/6-31G(d) method. The mean linear polarizability and mean first hyperpolarizability

properties of **III** were obtained from molecular polarizabilities based on theoretical calculations. In addition, frontier molecular orbitals (FMOs) and thermodynamic parameters for the title compound were performed with B3LYP/6-31G(d) the optimized structure.

## Results and discussion

### Description of the crystal structure

The crystal structure of **III** is monoclinic and space group  $P2_1/c$ ,  $M_w = 221.28$ ,  $a = 9.7879$  (8) Å,  $b = 7.9071$  (5) Å,  $c = 13.8045$  (10) Å,  $\beta = 102.266$  (6), and  $V = 1043.99(13)$  Å<sup>3</sup>,  $D_x = 1.408$  g/cm<sup>-3</sup>. Additional information for the structure determinations are given in Table S1. The dihedral angle between the benzene and triazole rings is 85.33 (6)°, indicating that these two rings are almost orthogonal to each other. Similarly, the plane of the ethyl moiety (N3/C9/C10) is twisted by 89.71 (8)° out of the mean plane of the triazole ring. There is one weak intramolecular C—H...S interaction (Fig. S1), forming a five-membered ring fused with the triazole ring. Intermolecular N2—H2...S1<sup>ii</sup> hydrogen bonding (Table 3) results in the formation of a dimeric structure.

Intermolecular O—H...N and C—H... $\pi$  interactions (Table 3) link the molecules into an infinite two-dimensional network (Cg1 in Table 3 is the centroid of the triazole ring). Intermolecular weak  $\pi$ - $\pi$  stacking interactions between the benzene ring and its symmetry-related partner at (1 - x, -y, -z) are also observed along the b axis, with a distance of 3.906 (2) Å between the ring centroids and a perpendicular distance between the rings of 3.556 (2) Å.

Previously, we have reported the closely related compound 3-(2-hydroxyphenyl)-4-phenyl-H-1,2,4-triazole-5(4H)-thione, (**VIII**) [57], which differs only in the 4-position (ethyl versus phenyl). When the bond lengths and angles of the triazole rings in (**III**) and (**VIII**) are compared, it is seen that the values are very close to each other. However, the C1—C3 bond length of 1.4731 (14) Å in (**III**) is significantly longer than the corresponding value in (**VIII**), 1.458 (2) Å. This difference may be due to a shortening of the C1—C3 bond length in (**III**) caused by O—H...N and C—H... $\pi$  intramolecular interactions.

### Optimized geometry

The optimized parameters like bond lengths, bond angles, and dihedral angles of **III** were taken by using the B3LYP/6-31G(d) method. The atomic numbering design of the theoretical geometric structure is given in Fig. 3b. The geometric parameters which accounted with the experimental data from the study are listed in Table 4. The slight conformational discrepancies are observed between the X-ray structure of **III** and its optimized counterparts (see Fig. S2). It is clear that the experimental results and the theoretical calculations are for the solid phase and for the gas phase sequentially. The existence of a crystal field along with the intermolecular interactions connects the molecules together, which results with some differences in bond parameters between

the calculated and experimental values in solid state. The orientation of the triazole ring of **III** proved the most notable discrepancy, and is defined with torsion angle C2—N2—N1—C1 [-0.922(13)°], which is calculated at -0.878 °C for B3LYP/6-31G(d) level.

The structures obtained from theoretical calculations is globally compared through a logical method that superimposes molecular skeleton with what obtained from X-ray diffraction, which in conclusion gives a RMSE of 0.403 Å for B3LYP/6-31G(d) (Fig. S2). This magnitude of RMSE can be explained by the fact that the intermolecular Coulombic interaction with the neighboring molecules are absent in gas phase, whereas the experimental result corresponds to interacting molecules in the crystal lattice [58].

### IR spectroscopy

DFT/B3LYP method with 6-31G(d) basis set was used for calculating harmonic vibrational frequencies of **III**, and Gauss-View molecular visualization program for the vibrational band assignments. The vibrational frequencies were analyzed for facilitating the assignment of the observed peaks and the results of our calculation for **III** were compared with the experimental results (Table 5). The consistency of the experimental results with our calculations gives good conclusions in general.

Fig. 4 shows its results. The OH group vibrations are found to be the possibly most sensitive to environment, therefore they show pronounced shifts in the spectra of the hydrogen-bonded species. The optimum absorption region of non-hydrogen-bonded or a free hydroxyl group is 3550–3700 cm<sup>-1</sup> region [59]. In case of their presence in molecule, intra- and intermolecular hydrogen bonding reduces O—H stretching band to 3000–3550 cm<sup>-1</sup> region [60]. The IR spectra of **III** with an intense and relatively sharp band at maximum 3216 cm<sup>-1</sup> was assigned to the stretching vibrations of the sub-group in the intermolecular O—H...N hydrogen bonds formed between N1 atom and O atom of hydroxyl group. This band has been calculated at 3606 cm<sup>-1</sup> for B3LYP level.

In the literature, some N—H stretching modes observed for the different substituent-triazole ring are 3383 cm<sup>-1</sup> [61] and 3417 cm<sup>-1</sup> [62] as experimentally. In our study, the N—H stretching mode was observed at 3390 cm<sup>-1</sup> which has a red shift and the cause of this shift is the intermolecular N2—H2...S1 hydrogen bonding. The red shifting is further enhanced by the reduction in the N—H bond order values, occurring due to donor-acceptor interaction [63]. These differences of O—H (390 cm<sup>-1</sup>) and N—H stretching vibrations (141 cm<sup>-1</sup>) occurred between the results of the experimental and calculations are due to the consideration of the isolated molecules (in gas phase) in the calculational method.

The aromatic C—H stretching, C—H in-plane bending and C—H out-of-plane bending vibrations appear in 2900–3150 cm<sup>-1</sup>, 1100–1500 cm<sup>-1</sup> and 700–1000 cm<sup>-1</sup> frequency ranges, respectively. The C—H aromatic stretching mode was observed at 3102 cm<sup>-1</sup> experimentally, and calculated at 3049–3099 cm<sup>-1</sup> for B3LYP. The bands at 3040 and 2983 cm<sup>-1</sup> correspond to the asymmetric stretching CH<sub>2</sub> and CH<sub>3</sub> modes, respectively. The C—H in-plane bending vibrations computed at 1445, 1386 and 1250 cm<sup>-1</sup> by B3LYP/6-31G(d) method shows excellent agreement with FT-IR bands at 1480, 1390 and 1230 cm<sup>-1</sup>. The theoretically computed values of the angles bending vibration modes show good agreement with the experimental values. The other vibrational frequencies can be seen in Table 5.

### NMR spectra

B3LYP method with 6-31G(d) basis set was used in order to calculate GIAO <sup>1</sup>H and <sup>13</sup>C chemical shift values (with respect to TMS), which then compared with the experimental <sup>1</sup>H and <sup>13</sup>C

**Table 3**  
Hydrogen bonding geometry (Å, °) for the title compound.

D—H...A	D—H	H...A	D...A	D—H...A
C9—H9B...S1	1.00 (2)	2.86 (2)	3.2386 (12)	104 (1)
O1—H1...N1 <sup>(i)</sup>	0.85 (2)	1.98 (2)	2.8227 (12)	175 (2)
N2—H2...S1 <sup>(iii)</sup>	0.90 (2)	2.38 (2)	2.2789 (10)	174 (2)
C9—H9B...Cg1 <sup>(iii)</sup>	1.00 (2)	2.76 (2)	3.4652 (13)	128 (1)

Symmetry code: (i) 1 - x, 1/2 + y, 1/2 - z, (ii) 2 - x, -y, 1 - z, (iii) 2 - x, 1/2 + y, 1/2 - z.

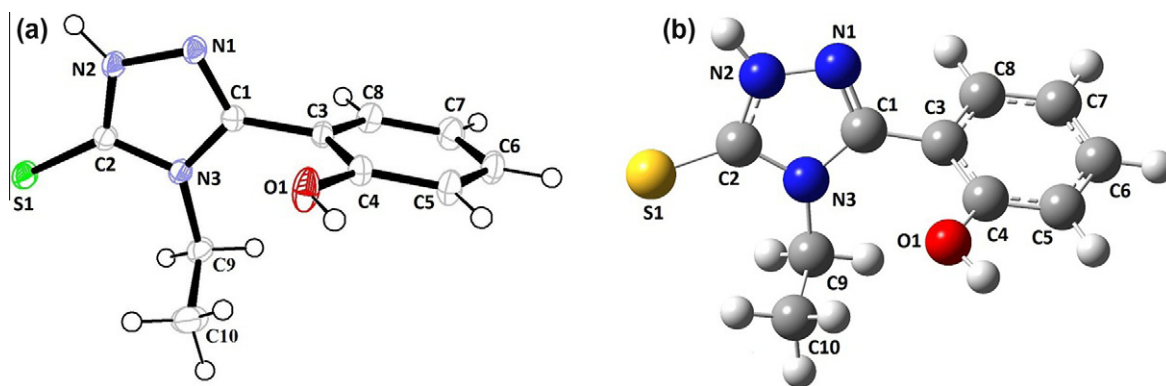


Fig. 3. (a) Ortep-3 diagram of the title compound and (b) the theoretical geometric structure of the title compound (with B3LYP/6-31G(d) level).

Table 4  
Selected molecular structure parameters.

Parameters	Experimental	B3LYP/6-31G(d)
<i>Bond lengths (Å)</i>		
N(1)–C(1)	1.3076 (13)	1.309
N(1)–N(2)	1.3737 (13)	1.366
N(2)–C(2)	1.3376 (14)	1.360
N(3)–C(2)	1.3688 (13)	1.385
N(3)–C(1)	1.3705 (13)	1.389
N(3)–C(9)	1.4694 (13)	1.467
RMSE <sup>a</sup>		0.013
<i>Bond angles (°)</i>		
C(1)–N(1)–N(2)	104.20 (9)	103.86
C(2)–N(2)–N(1)	113.06 (9)	114.57
C(2)–N(3)–C(1)	108.20 (8)	108.08
N(1)–C(1)–N(3)	110.71 (9)	111.18
N(2)–C(2)–N(3)	103.81 (9)	102.30
RMSE <sup>a</sup>		0.489
<i>Dihedral angles (°)</i>		
N(3)–C(1)–C(3)–C(8)	83.54 (13)	118.45
C(1)–N(3)–C(9)–C(10)	88.49 (13)	110.10

<sup>a</sup> Between the bond lengths and the bond angles computed by the theoretical method and those obtained from X-ray diffraction.

chemical shift values. Table 6 shows the results of the aforementioned calculation.

We have calculated <sup>1</sup>H chemical shift values (with respect to TMS) of 8.83–0.84 ppm at B3LYP/6-31G(d) level, whereas the experimental results are observed to be 13.80–1.03 ppm. The triplet observed at 3.42 ppm is assigned to C(9)H<sub>2</sub> and quartet observed at 1.03 ppm is assigned to C(10)H<sub>3</sub> that have been calculated at 3.33–3.90 and 0.84–1.77 ppm. The aromatic protons resonate at 7.14–7.82 ppm multiplet experimentally, that have been calculated at 6.72–7.48 ppm. In different substituent-1,2,4-triazole, the H chemical shift of N–H were observed to be 11.33–13.56 ppm [64]. The NH hydrogen of the 1,2,4-triazole ring appears at 13.80 ppm, and is determined computationally at 8.83 ppm. The signal assigned to proton of the OH is observed at 10.00 ppm. This was calculated 4.72 ppm at B3LYP level. In previous work, it was observed that chemical shift of O–H and N–H protons with the value of 10.45 ppm exist in the same band but these signals have been calculated as 5.56 and 9.64 ppm for 6-31G(d) level, respectively [65]. Because the intermolecular hydrogen bonds in molecular structure of **III** are neglected in the calculations, we can say that this difference between experimental and calculated chemical shifts is due to N–H···S and O–H···N intermolecular interactions.

We have calculated <sup>13</sup>C chemical shift values (with respect to TMS) of 13.37–164.32 ppm with B3LYP/6-31G(d), while, the experimental results were observed to be 15.10–182.33 ppm. As can be seen from Table 6, theoretical <sup>1</sup>H and <sup>13</sup>C chemical shift results of

Table 5  
Comparison of the experimental and calculated vibrational frequencies (cm<sup>-1</sup>).

Assignments	Experimental IR with KBr	B3LYP/6-31G(d)
$\nu$ (O–H)	3216	3606
$\nu$ (N–H)	3390	3531
$\nu_s$ Phenol (C–H)	3102	3099
$\nu_{as}$ Phenol (C–H)		3087
$\nu_{as}$ Phenol (C–H)		3076
$\nu_{as}$ Phenol (C–H) + $\nu_{as}$ ethyl (C–H)		3050
$\nu_{as}$ Phenol (C–H) + $\nu_{as}$ ethyl (C–H)	3040	3049
$\nu_{as}$ Ethyl (C–H)	2983	3021
$\nu_{as}$ Ethyl (C–H)		3013
$\nu_s$ Ethyl (C–H)	2950	2965
$\nu_s$ Ethyl (C–H)		2950
$\nu$ (C=C)	1640	1606
$\nu$ (C=C)		1586
$\nu$ (C=N) + $\nu$ (C=C)	1622	1541
$\alpha$ (C–H) of ethyl	1490	1482
$\alpha$ (C–H) of ethyl		1463
$\gamma$ (C–H) of phenol	1480	1445
$\gamma$ (C–H) + $\alpha$ (C–H) + $\gamma$ (N–H)		1439
$\gamma$ (C–H) + $\omega$ (C–H) + $\gamma$ (N–H)	1390	1386
$\omega$ (C–H) of ethyl + $\gamma$ (N–H)	1340	1353
$\gamma$ (C–H) of phenol + $\gamma$ (O–H)		1323
$\delta$ (C–H) of ethyl	1300	1318
$\gamma$ (C–H) of phenol + $\nu$ (C–O)	1230	1250
$\omega$ (C–H) of ethyl + $\nu$ (C–N–C)	1150	1190
$\nu$ (C=S)	1140	1130
$\delta$ (C–H) of ethyl + $\nu$ (N–N)		1071
$\nu$ (C–C) of phenol		1022
$\nu$ (C–C) of ethyl		946
$\nu$ (C–C) of ethyl + $\delta$ (C–H)		941
$\delta$ (C–H)	740	823
$\delta$ (C–C–C) of phenol		726
$\delta$ (C–N–C) + $\delta$ (C–C–C)		703
$\delta$ (N–C–S)		657

$\nu$ , Stretching;  $\alpha$ , scissoring;  $\gamma$ , rocking;  $\omega$ , wagging;  $s$ , symmetric;  $as$ , asymmetric;  $\beta$ , bending;  $\delta$ , of out plane bending.

the title compound are generally closer to the experimental chemical shift data.

#### Energetics and dipole moments

Calculations were conducted in five solvents ( $\epsilon = 78.36$ , H<sub>2</sub>O;  $\epsilon = 46.83$ , DMSO;  $\epsilon = 24.85$ , C<sub>2</sub>H<sub>5</sub>OH;  $\epsilon = 10.13$ , CH<sub>2</sub>ClCH<sub>2</sub>Cl;  $\epsilon = 4.71$ , CHCl<sub>3</sub>) in order to evaluate the total energy and dipole moment behavior of **III** in solvent media, which was conducted at B3LYP/6-31G(d) level using the Onsager and PCM methods. Table S2 shows the results of the aforementioned calculation. It

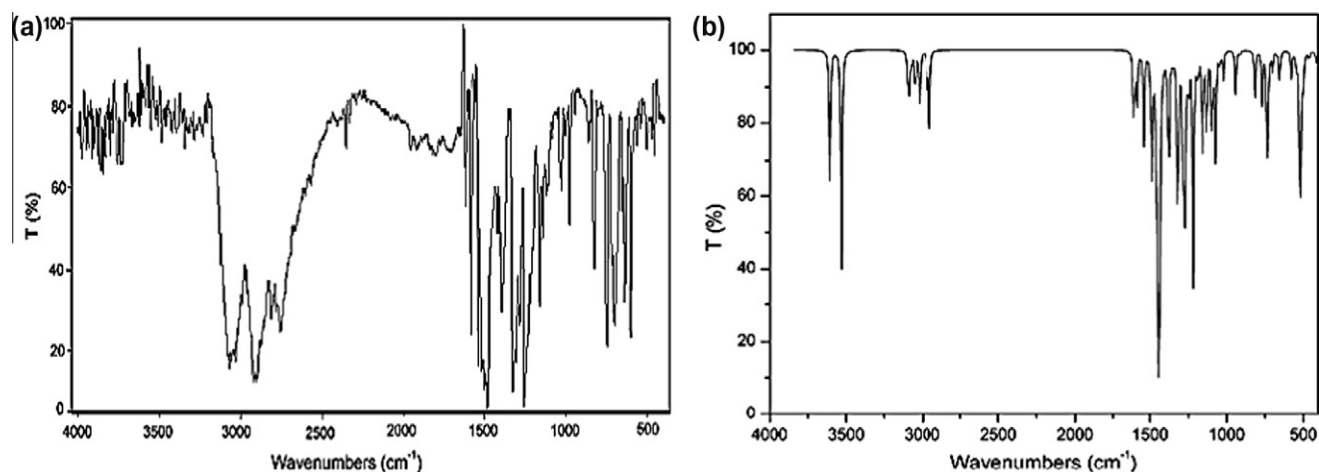


Fig. 4. (a) FT-IR spectrum of the title compound and (b) simulated B3LYP level IR spectra.

Table 6

Theoretical and experimental  $^1\text{H}$  and  $^{13}\text{C}$  isotropic chemical shifts (with respect to TMS, all values in ppm) for the title compound.

Atom	Experimental (ppm) (DMSO- $d_6$ )	Calculated (ppm) B3LYP/6-31G(d)
C1	160.13	146.20
C2	182.33	164.32
C3	115.45	107.43
C4	168.1	148.92
C5	117.88	109.52
C6	135.51	127.56
C7	116.01	114.40
C8	134.77	127.63
C9	45.04	42.71
C10	15.10	13.37
3H ( $\text{CH}_3$ )	1.03	0.84, 1.61 and 1.77
2H ( $\text{CH}_2$ )	3.47	3.33 and 3.90
4H ( $\text{Ar}-\text{CH}$ )		7.14–7.82
6.72–7.48		
1H ( $\text{NH}$ )	13.80	8.83
1H ( $\text{O}-\text{H}$ )	10.00	4.72

can be inferred from the table that an increase in the polarity of the solvent decreases the total energy amount that **III** obtains, which therefore increases the stability of **III**. Fig. S3 shows the energy difference between gas phase and solvent media. It can be observed in Fig. S3 that PCM method provides more stable structure than Onsager's method (6.45778 kcal/mol average). On the other hand, that trend in total energies was not observed in dipole moments. The dipole moments calculated using the Onsager method are larger than those calculated with PCM method in various solvents, and an increase in solvent polarity causes also an increase in the dipole moments obtained for the two solvation methods. Solvent effects improve the charge present delocalized in molecules, therefore, causes dipole moments to rise. One of the important factor in measuring solvent effect is ground-state dipole moment; a large ground-state dipole moment strongly increases the effects of solvent polarity [66,67].

#### Atomic charge distributions in gas-phase and in solution-phase

Mulliken atomic charge calculation has an important role in the application of quantum chemical calculation to molecular system because of atomic charges effect dipole moment, molecular polarizability, electronic structure and a lot of properties of molecular

systems. The charge distributions over the atoms suggest the formation of donor and acceptor pairs involving the charge transfer in the molecule. The Mulliken atomic charges for the non-H atoms of **III** calculated at the B3LYP/6-31G(d) level in gas-phase are presented in Table S3. To investigate the solvent effect for the atomic charge distributions of **III**, based on the B3LYP/6-31G(d) model and PCM method, three solvents (chloroform, ethanol and water) were selected and calculated values were also listed in Table S3.

The Mulliken atomic charges show that the N1, N2 and N3 atoms of triazole ring, O1 atom of hydroxyl group and S1 atom have larger negative atomic charges in the gas phase. On the other hand, it is found that, in solution-phase, the atomic charge values of the N1, S1 and O1 atoms are larger than those in gas-phase and while their atomic charge values will increase with the increase of the polarity of the solvent, that value of N2 and N3 decrease with the increasing polarity of the solvent. The coordination of these atoms will change in different solvents, which may be helpful when one wishes to use **III** to construct interesting metal complexes with different coordinate geometries [68]. This calculated result is not only consistent with many reported experimental values [69–71], it also supports the original idea of our synthesis.

#### Molecular electrostatic potential

Molecular electrostatic used extensively for interpreting potentials have been and predicting the reactive behavior of a wide variety of chemical system in both electrophilic and nucleophilic reactions, the study of biological recognition processes and hydrogen bonding interactions [72].

$V(\mathbf{r})$ , at a given point  $\mathbf{r}(x, y, z)$  in the vicinity of a molecule, is defined in terms of the interaction energy between the electrical charge generated from the molecule electrons and nuclei and positive test charge (a proton) located at  $\mathbf{r}$ . Unlike many of the other quantities used at present and earlier as indices of reactivity,  $V(\mathbf{r})$  is a real physical property that can be determined experimentally by diffraction or by computational methods. For the systems studied the MEP values were calculated as described previously, using the equation [73]:

$$V(\mathbf{r}) = \sum \frac{Z_A}{|\mathbf{R}_A - \mathbf{r}|} - \int \frac{\rho(\mathbf{r}')}{|\mathbf{r}' - \mathbf{r}|} d\mathbf{r}'$$

where the summation runs over all the nuclei  $A$  in the molecule and polarization and reorganization effects are neglected.  $Z_A$  is the charge of the nucleus  $A$ , located at  $\mathbf{R}_A$  and  $\rho(\mathbf{r}')$  is the electron density function of the molecule. To predict reactive sites for electrophilic

and nucleophilic attack for the investigated molecule, molecular electrostatic potential (MEP) was calculated at B3LYP/6-31G(d) optimized geometries. Red and blue areas in the MEP map refer to the regions of negative and positive potentials and correspond to the electron-rich and electron-poor regions, respectively, whereas the green color signifies the neutral electrostatic potential. The MEP surface provides necessary information about the reactive sites.

The negative regions  $V(r)$  were related to electrophilic reactivity and the positive ones to nucleophilic reactivity. As easily can be seen in Fig. 5, this molecule has several possible sites for electrophilic attack in which  $V(r)$  calculations have provided in-sights. Negative regions in the studied molecule were found around the O1 atom and N1 atom of triazole ring. The negative  $V(r)$  values are  $-0.045$  a.u. for O1 atom, which is the most negative region,  $-0.038$  a.u. for N1 atom which is a less negative region. However, a maximum positive region is localized on the H atom of the hydroxyl group with a value of  $+0.080$  a.u. indicating a possible site for nucleophilic attack. According to these calculated results, the MEP map shows that the negative potential sites are on electronegative atoms as well as the positive potential sites are around the hydrogen atoms. These sites give information about the region from where the compound can have intermolecular interactions.

### Conformational analysis

To define the preferential positions of phenol ring and ethyl group, a preliminary search of low energy structures was performed

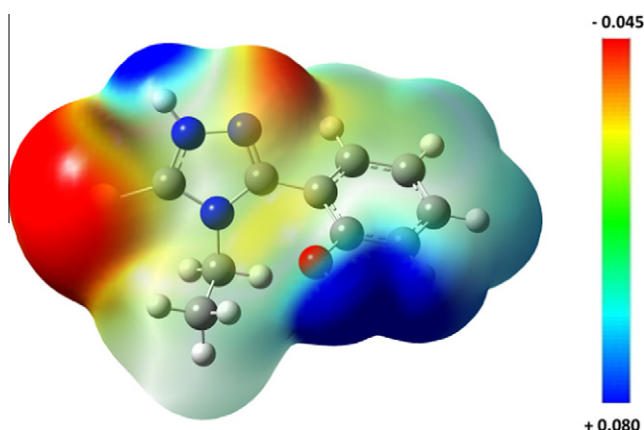


Fig. 5. Molecular electrostatic potential map calculated at B3LYP/6-31G(d) level.

with B3LYP method using 6-31G basis set as a function of the selected degrees of torsional freedom,  $\varphi_1(\text{N3—Cl—C3—C8})$  and  $\varphi_2(\text{C10—C9—N3—C1})$ . The respective values of the selected degrees of torsional freedom,  $\varphi_1(\text{N3—Cl—C3—C8})$  and  $\varphi_2(\text{C10—C9—N3—C1})$ , are in optimized geometries  $-118.449$  and  $-110.102^\circ$ , respectively for B3LYP/6-31G(d).

The molecular 1-D energy profiles with respect to rotations about the selected torsion angles are presented in Fig. 6. According to the results, the low-energy domains for  $\varphi_1(\text{N3—Cl—C3—C8})$  are located at  $-130$  and  $+120^\circ$ , with energies of  $-1025.356$  and  $-1025.355$  a.u., respectively, while they are located at  $-80$  and  $+110^\circ$  having energy of  $-1025.356$  and  $-1025.355$  a.u., respectively, for  $\varphi_2(\text{C10—C9—N3—C1})$ . Energy difference between the most favorable and unfavorable conformers, which arises from rotational potential barrier calculated with respect to the selected torsion angles, were calculated as  $7.185 \text{ kcal/mol}^{-1}$  for B3LYP/6-31G(d).

### Frontier molecular orbitals

In principle, there are several ways to calculate the excitation energies. The simplest one involves the difference between the highest occupied molecular orbital (HOMO) and the lowest unoccupied molecular orbital (LUMO) of a neutral system, which is a key parameter in determining molecular properties [74]. Moreover, the Eigen values of HOMO ( $\pi$  donor) and LUMO ( $\pi$  acceptor) and their energy gap reflect the chemical activity of the molecules. Recently, the energy gap between HOMO and LUMO has been used to prove the bioactivity from intramolecular charge transfer (ICT) [75,76]. Fig. 7 shows the distributions and energy levels of the HOMO-1, HOMO, LUMO and LUMO+1 orbitals computed at the B3LYP/6-31G(d) level for **III**. As seen from Fig. 7, both in the HOMO and HOMO-1, electrons are delocalized on the S1 atom and triazole ring. For the LUMO and LUMO+1 electrons are mainly delocalized on the triazole and phenol rings. The value of the energy separation between the HOMO and LUMO is  $4.371 \text{ eV}$ . This large HOMO-LUMO gap automatically means high excitation energies for many of excited states, a good stability and a high chemical hardness for **III**.

### Nonlinear optical effects

NLO properties has been of great interest by the recent years. Because some synthesized novel materials show efficient nonlinear optical that are used telecommunication, potential applications in

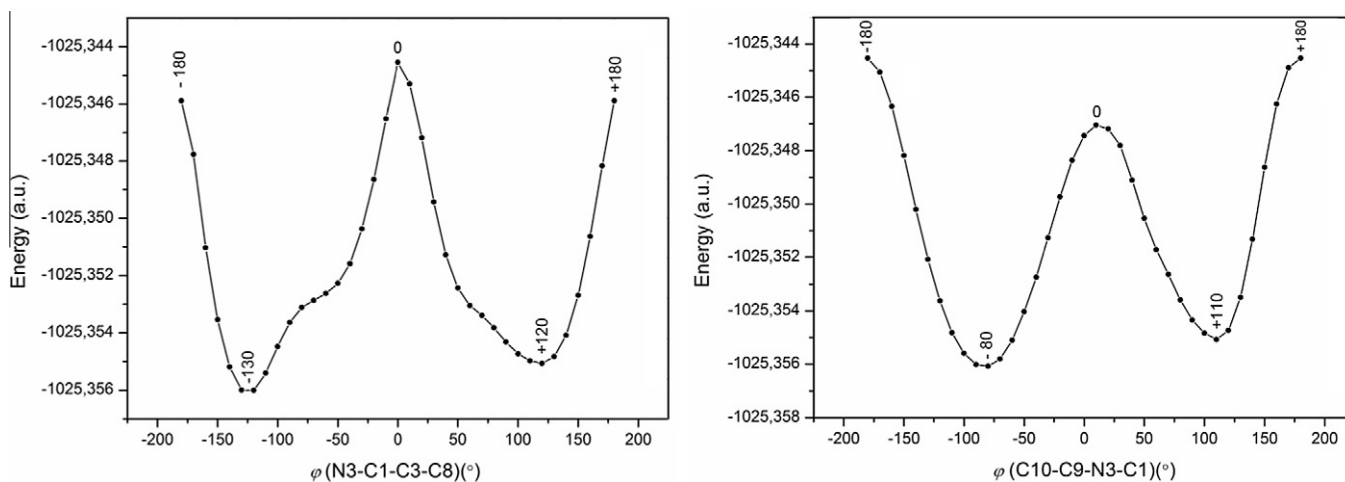


Fig. 6. Molecular energy profile against the selected torsional degree of freedom at B3LYP/6-31G(d) level.

modern communication technology, optical signal processing and data storage.

The text previously explains the way that total molecular dipole moment ( $\mu$ ), linear polarizability ( $\alpha$ ) and first-order hyperpolarizability ( $\beta$ ) are calculated using Gaussian output in detail [77]. DFT has been commonly used as an effective method to investigate organic NLO materials. Literature extensively states that electric hyperpolarizability can reliably be calculated through the B3LYP approach reliable values in, compared to accuracies of traditional *ab initio* methods. It is also reported that most computational scientists are interested in this aforementioned predictive capability of widely used B3LYP method [78,79]. In addition, this study preferred the basis set 6-31G(d) for the calculations of the hyperpolarizability, considering its reliability and the required computational time [80].

The electronic dipole moment  $\mu_i$  ( $i = x, y, z$ ), polarizability  $\alpha_{ij}$  and the first hyperpolarizability  $\beta_{ijk}$  of **III** were calculated at the B3LYP/6-31G(d) level using Gaussian 09W program package. Urea is one of the prototypical molecules used in the study of the NLO properties of molecular systems. Therefore it was used frequently as a threshold value for comparative purposes. The calculated values of  $\alpha_{tot}$  and  $\beta_{tot}$  for **III** are, 21.264 Å<sup>3</sup> and  $5.727 \times 10^{-30}$  cm<sup>5</sup>/esu, which are greater than those of urea (the  $\alpha_{tot}$  and  $\beta_{tot}$  of urea are 3.831 Å<sup>3</sup> and  $0.37 \times 10^{-30}$  cm<sup>5</sup>/esu obtained by B3LYP/6-31G(d) method). According to the magnitude of the first hyperpolarizability, **III** may be a potential applicant in the development of NLO materials.

#### Biological study

##### Antibacterial and antifungal activity

The investigation of antibacterial and antifungal screening data revealed that the title compound showed good inhibition at 1.56–25 mg/mL in DMSO. The screening result indicate that title compound tested exhibited significant antibacterial and antifungal activities when compared with the reference drug. The title compound was found to be same potent as the reference drug, ciprofloxacin, in case of *E. coli*. Structure and biological activity relationship of title compound showed that presence of 4-hydroxy groups attached to phenyl ring to the triazole ring of the title compound is responsible for good antimicrobial activity [81]. In conclusion the present study showed that the synthesized compound can be used as template for future development through modification and derivatization to design more potent and selective antimicrobial agents.

##### Antioxidant activity

Since the antioxidants are gaining a lot of importance as panacea for a large number of life-style diseases like aging, cancer, diabetes, cardiovascular and other degenerative diseases, it is of immense significance to establish some new antioxidants by a convenient synthetic methodology.

Although a number of methods such as ORAC, ABTS, DMPD, FRAP, TRAP, TBA, superoxide radical scavenging, hydroxyl radical scavenging, nitric oxide radical scavenging, xanthine oxidase, cytochrome C, reducing power method, etc. available, the DPPH method is very common and proved as the best [82].

It has been reported that the antioxidant activity of the phenolic compounds depends on their molecular structure, especially on their hydrogen-donating ability and subsequent stabilization of the formed phenoxy radical [83]. As shown in Table 7, the title compound has scavenging activity between 40.9% and 88.1% within the investigated concentration range. The antioxidant activity of the title compound is obvious that the scavenging activity increases with increasing sample concentration in the range tested. This activity can be explained on the basis of their structure as

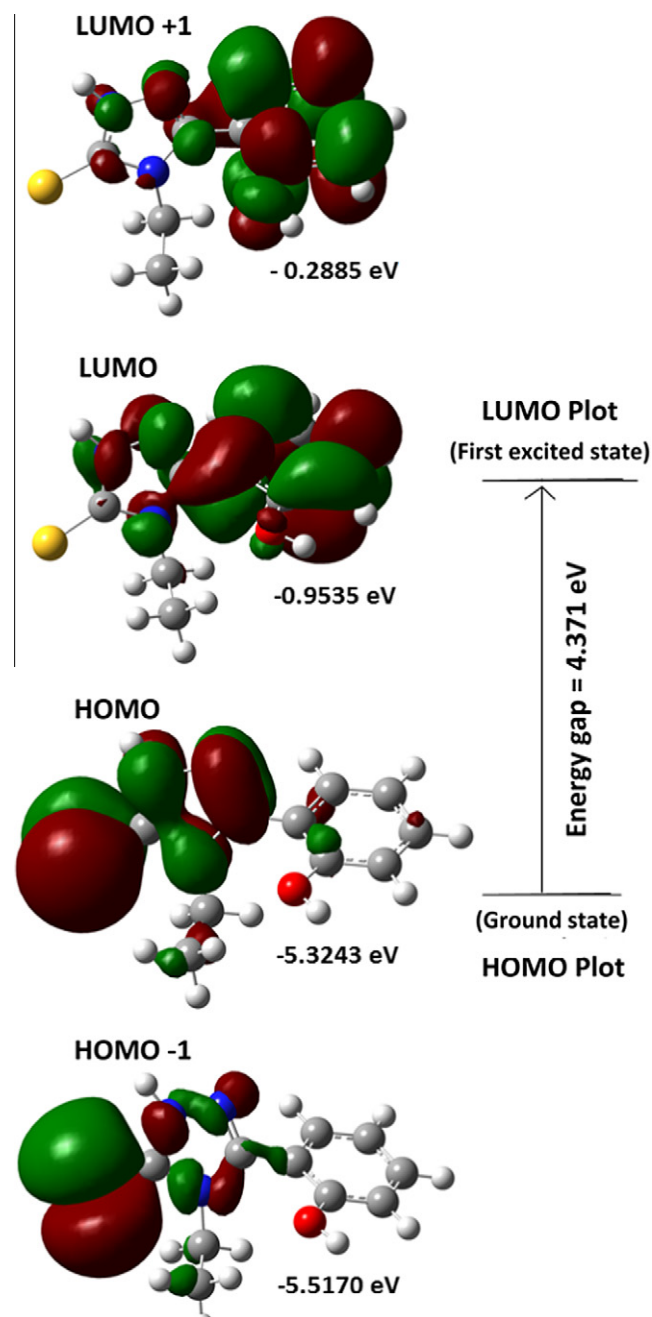


Fig. 7. Molecular orbital surfaces and energy levels given in parentheses for the HOMO, HOMO–1, LUMO and LUMO+1 of the title compound computed at B3LYP/6-31G(d) level.

Table 7

Antioxidant scavenging activity data of the title compound on DPPH<sup>•</sup> free radical at different concentrations.

Tested compound	DPPH scavenging activity (%)				
	62.5 μM	125 μM	187.5 μM	250 μM	312.5 μM
Title compound	40.9 ± 0.4	55.2 ± 0.1	66.0 ± 0.3	75.5 ± 0.1	88.1 ± 0.1
Ascorbic acid <sup>a</sup>	55.0 ± 0.2	65.0 ± 0.2	75.0 ± 0.2	85.0 ± 0.2	95.0 ± 0.2

<sup>a</sup> Ascorbic acid, was used as a standard.

these derivatives possess phenolic hydroxyls which are available as hydrogen donors to the DPPH radical.

## Conclusions

The investigation of the present work is illuminate the spectroscopic properties such as molecular parameters, frequency assignments and magnetic properties of title compound by using FT-IR,  $^1\text{H}$  and  $^{13}\text{C}$  NMR techniques and tools derived from the density functional theory. A conformational analysis was carried out by means of molecular dynamics simulations. Due to the lack of experimental information on the structural parameters available in the literature, the optimized geometric parameters (bond lengths and bond angles) was theoretically determined at B3LYP/6-31G(d) level of theory and compared with the structurally similar compounds. The X-ray structure is found to be very slightly different from its optimized counterpart, and the crystal structure is stabilized by N—H...S and O—H...N hydrogen bonds. It was noted here that the experimental results belong to solid phase and theoretical calculations belong to gaseous phase. In the solid state, the existence of the crystal field along with the intermolecular interactions have connected the molecules together, which result in the differences of bond parameters between the calculated and experimental values. Despite the differences observed in the geometric parameters, the general agreement is good and the theoretical calculations support the solid-state structure. The vibrational FT-IR spectrum of the **III** was recorded and computed vibrational wavenumbers. The magnetic properties of the title molecule were observed and calculated the same method. The chemical shifts were compared with experimental data in DMSO solution, showing a very good agreement both for  $^{13}\text{C}$  and  $^1\text{H}$  chemical shifts. The total energy of **III** decrease with the increasing polarity of the solvent and the stability of **III** increase in going from the gas phase to the solution phase. When all theoretical results scanned, they are showing good correlation with experimental data. The antimicrobial activity study revealed that the title compound showed good antibacterial and antifungal activities against pathogenic strains. The antioxidant activity of the title compound is obvious that the scavenging activity increases with increasing sample concentration in the range tested.

## Appendix A. Supplementary material

Supplementary data associated with this article can be found, in the online version, at <http://dx.doi.org/10.1016/j.saa.2012.12.052>.

## References

- [1] F.R. Benson, Tetrazoles, tetrazines and purines and related ring systems, in: R.C. Elderfield (Ed.), *Heterocyclic Compounds*, vol. 8, Wiley, New York, 1967, pp. 1–104.
- [2] C. Jr, Temple, Triazoles 1, 2, 4, in: J.A. Montgomery (Ed.), *Chemistry of the Heterocyclic Compounds*, vol 37, Wiley, New York, 1981, pp. 155–162.
- [3] P.C. Unangst, G.P. Shrum, D.T. Connor, R.D. Dyer, D.J. Schrier, *J. Med. Chem.* 35 (1992) 3691–3698.
- [4] M.D. Mullican, M.W. Wilson, D.T. Conner, C.R. Kostlan, D.J. Schrier, R.D. Dyer, *J. Med. Chem.* 36 (1993) 1090–1099.
- [5] D.H. Jones, R. Slack, S. Squires, K.R.H. Wooldridge, *J. Med. Chem.* 8 (1965) 676–680.
- [6] J.K. Sughen, T. Yoloye, *Pharm. Acta Helv.* 58 (1978) 64–68.
- [7] S.A. Shams El-Dine, A.A.B. Hazzaa, *Pharmazie* 29 (1974) 761–763.
- [8] M.R. Stillings, A.P. Welbourn, D.S. Walter, *J. Med. Chem.* 29 (1986) 2280–2284.
- [9] K. Sztanke, T. Tuzimski, J. Rzymowska, K. Pasternak, M. Kandefer-Szerszeń, *Eur. J. Med. Chem.* 43 (2008) 404–419.
- [10] K. Ilango, P. Valentina, *Pharm. Chem.* 2 (2010) 16–22.
- [11] N. Demirbaş, D. Ugurluoglu, A. Demirbaş, *Bioorg. Med. Chem.* 10 (2002) 3717–3723.
- [12] J.M. Kane, M.W. Dudley, S.M. Sorensen, F.P. Miller, *J. Med. Chem.* 31 (1988) 1253–1258.
- [13] R.D. Porsolt, A. Bertin, M. Jalfre, *Arch. Int. Pharmacodyn. Ther.* 229 (1977) 327–336.
- [14] A. Vamvakides, *Ann. Pharm. Fr.* 48 (1990) 154–159.
- [15] W. Vreugdenhil, J.G. Haasnoot, J. Reedijk, A.L. Spek, *Inorg. Chim. Acta* 129 (1987) 205–216.
- [16] G.A. van Albada, R.A.G. de Graaff, J.G. Haasnoot, J. Reedijk, *Inorg. Chem.* 23 (1984) 1404–1408.
- [17] G. Vos, R.A. le Febvre, R.A.G. de Graaff, J.G. Haasnoot, J. Reedijk, *J. Am. Chem. Soc.* 105 (1983) 1682–1683.
- [18] O. Kahn, C.J. Martinez, *Science* 279 (1998) 44–48.
- [19] D.Z. Wang, Q. Zhang, J.B. Zhang, Y.G. Wu, L.H. Cao, P.Y. Ma, *Polyhedron* 42 (2012) 216–226.
- [20] M. Koparir, A. Cetin, A. Cansiz, *Molecules* 10 (2005) 475–480.
- [21] N. Dege, N. Özdemir, A. Cetin, A. Cansiz, M. Sekerci, M. Dincer, *Acta Cryst. E* 61 (2005) o17–o19.
- [22] S. Ozturk, M. Akkurt, A. Cansiz, M. Koparir, M. Sekerci, F.W. Heinemann, *Acta Cryst. E* 60 (2004) o642–o644.
- [23] A. Cansiz, A. Cetin, P. Kutulay, M. Koparir, *Asian J. Chem.* 21 (2009) 617–626.
- [24] S.O. Yildirim, M. Akkurt, A. Cetin, A. Cansiz, M. Sekerci, F.W. Heinemann, *Anal. Sci., X-ray Structure Analysis Online* 21 (2005) x121–x122.
- [25] S.O. Yildirim, M. Akkurt, M. Koparir, A. Cansiz, M. Sekerci, F.W. Heinemann, *Acta Cryst. E* 60 (2004) o2368–o2370.
- [26] M. Ahmedzade, A. Cukurovali, M. Koparir, *J. Chem. Soc. Pakistan* 25 (2003) 51–55.
- [27] M. Koparir, A. Cansiz, M. Ahmedzade, A. Cetin, *Heteroatom Chem.* 15 (2004) 26–31.
- [28] O.F. Ozturk, A. Cansiz, M. Koparir, *Transit. Metal Chem.* 32 (2007) 224–227.
- [29] S. Ozturk, M. Akkurt, A. Cansiz, M. Koparir, M. Sekerci, F.W. Heinemann, *Acta Cryst. E* 60 (2004) o820–o821.
- [30] M. Koparir, A. Cansiz, A. Cetin, C. Kazaz, *Chem. Nat. Comp.* 41 (2005) 539–571.
- [31] N. Dege, A. Cetin, A. Cansiz, M. Sekerci, C. Kazaz, M. Dincer, O. Buyugungor, *Acta Cryst. E* 60 (2004) o1883–o1885.
- [32] M. Dincer, N. Özdemir, A. Cetin, A. Cansiz, M. Sekerci, *Acta Cryst. E* 61 (2005) o3214–o3216.
- [33] S. Genc, N. Dege, A. Cetin, A. Cansiz, M. Sekerci, M. Dincer, *Acta Cryst. E* 60 (2004) o1340–o1342.
- [34] F.D. Proft, P. Geerlings, *Chem. Rev.* 101 (2001) 1451–1464.
- [35] C. Orek, P. Koparir, M. Koparir, *Spectrochim. Acta A* 97 (2012) 923–934.
- [36] A. Cansiz, A. Cetin, C. Orek, M. Karatepe, K. Sarac, A. Kus, P. Koparir, *Spectrochim. Acta A* 97 (2012) 607–615.
- [37] H. Tanak, *Comput. Theor. Chem.* 967 (2011) 93–101.
- [38] G. Fitzgerald, J. Andzelm, *J. Phys. Chem.* 95 (1991) 10531–10534.
- [39] J. Andzelm, E. Wimmer, *J. Chem. Phys.* 96 (1992) 1280–1303.
- [40] A. Barry, Procedures and theoretical considerations for testing antimicrobial agents in agar media, in: Lorian (Ed.), *Antibiotics in Laboratory Medicine*, fifth ed., Williams and Wilkins, Baltimore, 1991 (MD, 1).
- [41] D.J. MacLowry, M.J. Jaqua, S.T. Selpak, *Appl. Microbiol.* 20 (1970) 46–53.
- [42] C.H. Fenlon, M.H. Cynaon, *Antimicrob. Agents Chemother.* 29 (1986) 386–388.
- [43] R. Davis, A. Markam, J.A. Balfour, *Drugs* 51 (1996) 1019–1074.
- [44] B.A. Arthington-Skaggs, M. Motley, D.W. Warnock, C.J. Morrison, *J. Clin. Microbiol.* 6 (2000) 2254–2260.
- [45] R.S. Verma, *Antifungal Agents: Past, Present and Future Prospects*, National Academy Of Chemistry and Biology, India, 1998.
- [46] M.M. Hossain, M.F. Aziz, R. Ahmed, M. Hossain, A. Mahmuda, T. Ahmed, M.H. Mazumder, *Int. J. Pharm. Sci.* 2 (2010) 60–63.
- [47] M.J. Frisch, G.W. Trucks, H.B. Schlegel, G.E. Scuseria, M.A. Robb, J.R. Cheeseman, G. Scalmani, V. Barone, B. Mennucci, G.A. Petersson, H. Nakatsuji, M. Caricato, X. Li, H.P. Hratchian, A.F. Izmaylov, J. Bloino, G. Zheng, J.L. Sonnenberg, M. Hada, M. Ehara, K. Toyota, R. Fukuda, J. Hasegawa, M. Ishida, T. Nakajima, Y. Honda, O. Kitao, H. Nakai, T. Vreven, J.A. Montgomery Jr., J.E. Peralta, F. Ogliaro, M. Bearpark, J.J. Heyd, E. Brothers, K.N. Kudin, V.N. Staroverov, R. Kobayashi, J. Normand, K. Raghavachari, A. Rendell, J.C. Burant, S.S. Iyengar, J. Tomasi, M. Cossi, N. Rega, J.M. Millam, M. Klene, J.E. Knox, J.B. Cross, V. Bakken, C. Adamo, J. Jaramillo, R. Comperts, R.E. Stratmann, O. Yazyev, A.J. Austin, R. Cammi, C. Pomelli, J.W. Ochterski, R.L. Martin, K. Morokuma, V.G. Zakrzewski, G.A. Voth, P. Salvador, J.J. Dannenberg, S. Dapprich, A.D. Daniels, O. Farkas, J.B. Foresman, J.V. Ortiz, J. Cioslowski, D.J. Fox, Gaussian, Inc., Wallingford CT, 2009.
- [48] H.B. Schlegel, *J. Comput. Chem.* 3 (1982) 214–218.
- [49] C. Peng, P.Y. Ayala, H.B. Schlegel, M.J. Frisch, *J. Comput. Chem.* 17 (1996) 49–56.
- [50] J.B. Foresman, A. Frisch, *Exploring Chemistry with Electronic Structure Methods*, second ed., Gaussian, Inc., Pittsburgh, 1996.
- [51] R. Dennington II, T. Keith, J. Millam, GaussView, Version 4.1.2, Semichem, Inc., Shawnee Mission, KS, 2007.
- [52] L. Onsager, *J. Am. Chem. Soc.* 58 (1936) 1486–1493.
- [53] S. Miertus, E. Scrocco, J. Tomasi, *Chem. Phys.* 55 (1981) 117–129.
- [54] V. Barone, M. Cossi, *J. Phys. Chem. A* 102 (1998) 1995–2001.
- [55] M. Cossi, N. Rega, G. Scalmani, V. Barone, *J. Comput. Chem.* 24 (2003) 669–681.
- [56] J. Tomasi, B. Mennucci, R. Cammi, *Chem. Rev.* 105 (2005) 2999–3093.
- [57] S. Genc, N. Dege, A. Cetin, A. Cansiz, M. Sekerci, M. Dincer, *Acta Cryst. E* 60 (2004) o1580–o1582.
- [58] H. Tanak, *J. Phys. Chem. A* 115 (2011) 13865–13876.
- [59] C.Y. Panicker, H.T. Varghese, K.R. Ambujakshan, S. Mathew, S. Ganguli, A.K. Nanda, C. Van Alsenoy, *J. Raman Spectrosc.* 40 (2009) 1262–1273.
- [60] A. Teimouri, A.N. Chermahini, K. Taban, H.A. Dabbagh, *Spectrochim. Acta A* 72 (2009) 369–377.
- [61] R. Ustabaş, N. Süleymanoğlu, H. Tanak, Y.B. Alpaslan, Y. Ünver, K. Sancak, *J. Mol. Struct.* 984 (2010) 137–145.
- [62] K. Sancak, Y. Ünver, H. Tanak, İ. Değirmençioğlu, E. Düğdü, M. Er, Ş. Işık, *J. Inclusion Phenom. Macrocycl. Chem.* 67 (2010) 325–334.

- [63] Y. Köysal, H. Tanak, *Spectrochim. Acta A* 93 (2012) 106–115.
- [64] P.J. Garratt, in: A.R. Katritzky, C.W. Rees, E.F.V. Scriven (Eds.), *Comprehensive Heterocyclic Chemistry II*, vol. 4, Elsevier Science Ltd., 1996, pp. 127–163.
- [65] T. Karakurt, M. Dincer, A. Cetin, M. Sekerci, *Spectrochim. Acta A* 77 (2010) 189–198.
- [66] A. Masternak, G. Wenska, J. Milecki, B. Skalski, S. Franzen, *J. Phys. Chem.* 109 (2005) 759–766.
- [67] Y. Le, J.F. Chen, M. Pu, *Int. J. Pharm.* 358 (2008) 214–218.
- [68] F.F. Jian, P.S. Zhao, Z.S. Bai, L. Zhang, *Struct. Chem.* 16 (2005) 635–639.
- [69] M. Baldini, M. Belicchi-Ferrari, F. Bisceglie, G. Pelosi, S. Pinelli, P. Tarasconi, *Inorg. Chem.* 42 (2003) 2049–2055.
- [70] L.J. Ashfield, A.R. Cowley, J.R. Dilworth, P.S. Donnelly, *Inorg. Chem.* 43 (2004) 4121–4123.
- [71] J.S. Casas, E.E. Castellano, J. Ellena, M.S. Garcia Tasende, A. Sanchez, J. Sordo, M.J. Vidarte, *Inorg. Chem.* 42 (2003) 2584–2595.
- [72] P. Politzer, J.S. Murray, Theoretical biochemistry and molecular biophysics: a comprehensive survey, Protein, in: D.L. Beveridge, R. Lavery (Eds.), *Electrostatic Potential Analysis of Dibenzo-p-dioxins and Structurally Similar Systems in Relation to their Biological Activities*, vol. 2, Adenine Press, Schenectady, NY, 1991 (Chapter 13).
- [73] P. Politzer, J. Murray, *Theor. Chem. Acc.* 108 (2002) 134.
- [74] M. Amalanathan, V.K. Rastogi, I.H. Joe, M.A. Palafox, R. Tomar, *Spectrochim. Acta A* 78 (2011) 1437–1444.
- [75] L. Padmaja, C. Ravi Kumar, D. Sajan, I.H. Joe, V.S. Jayakumar, G.R. Pettit, *J. Raman Spect.* 40 (2009) 419–428.
- [76] S. Sagdinc, H. Pir, *Spectrochim. Acta A* 73 (2009) 181–187.
- [77] K.S. Thanthirawatte, K.M. Nalin de Silva, *J. Mol. Struct. Theochem.* 617 (2002) 169–175.
- [78] G. Maroulis, D. Begue, C. Pouchan, *J. Chem. Phys.* 119 (2003) 794–798.
- [79] G. Maroulis, *J. Chem. Phys.* 129 (2008) 044314–044321.
- [80] C. Qin, Y. Si, G. Yang, Z. Su, *Comput. Theor. Chem.* 966 (2011) 14–19.
- [81] Q. Ding, L. Zhang, H. Zhang, *Phosphorus Sulfur* 185 (2010) 567–572.
- [82] V. Bondet, W. Brand-Williams, C. Berset, *Lebensm.-Wiss. Technol.* 30 (1997) 609–615.
- [83] F. Borges, F.A.M. Silva, C. Guimaraes, J.L.F.C. Lima, C. Matos, S. Reis, *J. Agric. Food Chem.* 48 (2000) 2122–2126.